



Stability Chart for the Delayed Mathieu Equation

Author(s): T. Insperger and G. Stepan

Source: *Proceedings: Mathematical, Physical and Engineering Sciences*, Vol. 458, No. 2024, (Aug. 8, 2002), pp. 1989-1998

Published by: The Royal Society

Stable URL: <http://www.jstor.org/stable/3067194>

Accessed: 16/06/2008 14:42

Your use of the JSTOR archive indicates your acceptance of JSTOR's Terms and Conditions of Use, available at <http://www.jstor.org/page/info/about/policies/terms.jsp>. JSTOR's Terms and Conditions of Use provides, in part, that unless you have obtained prior permission, you may not download an entire issue of a journal or multiple copies of articles, and you may use content in the JSTOR archive only for your personal, non-commercial use.

Please contact the publisher regarding any further use of this work. Publisher contact information may be obtained at <http://www.jstor.org/action/showPublisher?publisherCode=rsl>.

Each copy of any part of a JSTOR transmission must contain the same copyright notice that appears on the screen or printed page of such transmission.

JSTOR is a not-for-profit organization founded in 1995 to build trusted digital archives for scholarship. We enable the scholarly community to preserve their work and the materials they rely upon, and to build a common research platform that promotes the discovery and use of these resources. For more information about JSTOR, please contact support@jstor.org.

Stability chart for the delayed Mathieu equation

BY T. INSPERGER AND G. STÉPÁN

Department of Applied Mechanics, Budapest University of Technology and Economics, Budapest H-1521, Hungary (inspi@mm.bme.hu; stepan@mm.bme.hu)

*Received 15 January 2001; revised 15 October 2001; accepted 31 October 2001;
published online 7 June 2002*

In the space of system parameters, the closed-form stability chart is determined for the delayed Mathieu equation defined as $\ddot{x}(t) + (\delta + \varepsilon \cos t)x(t) = bx(t - 2\pi)$. This stability chart makes the connection between the Strutt–Ince chart of the Mathieu equation and the Hsu–Bhatt–Vyshnegradskii chart of the second-order delay-differential equation. The combined chart describes the intriguing stability properties of a class of delayed oscillatory systems subjected to parametric excitation.

Keywords: parametric excitation; time delay; stability

1. Introduction

Systems governed by time-periodic delay-differential equations often come up in different fields of science and engineering. One of the most important mechanical application is the dynamics of milling, where the regenerative effect of the cutting process causes the time delay, while the time-varying number of active teeth causes a time periodicity exactly equal to the time delay (see Insperger & Stépán 2000a; Davies *et al.* 2002; Bayly *et al.* 2001). A similar problem is the remote control of periodic robot motions, when the delay in the information transmission system is not negligible (see Insperger & Stépán 2000b). The qualitative investigation of these mechanical systems always includes stability analysis. This work can effectively be supported by the so-called stability charts.

The underlying mathematical problem of the above applications is the analysis of the delayed Mathieu equation. This is a special case of the linear periodic retarded functional differential equation (RFDE) of the general form

$$\dot{\mathbf{y}}(t) = \mathbf{L}(t, \mathbf{y}_t), \quad \mathbf{L}(t, \mathbf{y}_t) = \int_{-\tau}^0 d_{\vartheta} \boldsymbol{\eta}(t, \vartheta) \mathbf{y}(t + \vartheta), \quad \mathbf{L}(t + T, \mathbf{y}_t) = \mathbf{L}(t, \mathbf{y}_t). \quad (1.1)$$

The matrix $\boldsymbol{\eta}$ is a function of bounded variation on $[-\tau, 0]$ and the integral is a Stieltjes one, i.e. it describes discrete and continuous time delays as well. The linear functional \mathbf{L} can be represented in the above integral form according to the Riesz representation theorem (see Hale 1977), and the continuous function \mathbf{y}_t is defined by the shift

$$\mathbf{y}_t(\vartheta) = \mathbf{y}(t + \vartheta), \quad \vartheta \in [-\tau, 0]. \quad (1.2)$$

The Floquet theory (Floquet 1883) can be extended for these systems (see Hale & Lunel 1993; Farkas 1994). The linear operator $\mathbf{U}(t)$ defines the solutions by

$\mathbf{y}_t = U(t)\mathbf{y}_0$. While $U(t)$ plays the role of the fundamental matrix in classical Floquet theory, the role of the principal matrix is taken by $U(T)$. The non-zero elements of the spectrum of $U(T)$ are called the characteristic multipliers of system (1.1), also defined by

$$\text{Ker}(\mu\mathbf{I} - U(T)) \neq \emptyset. \quad (1.3)$$

Opposite to the classical case, periodic delayed systems usually have an infinite number of characteristic multipliers. If μ is a characteristic multiplier, and $\mu = \exp(\lambda T)$, then λ is called the characteristic exponent. Our investigation is based on the following two theorems (Hale & Lunel 1993).

Theorem 1.1. *The trivial solution of system (1.1) is asymptotically stable if and only if all the (infinite number of) characteristic multipliers are in modulus less than one, that is, all the characteristic exponents have negative real parts.*

Theorem 1.2. *$\mu = e^{\lambda T}$ is a characteristic multiplier of system (1.1) if and only if there exists a non-trivial solution in the form $\mathbf{y}(t) = \mathbf{p}(t)e^{\lambda t}$, where $\mathbf{p}(t) = \mathbf{p}(t + T)$.*

For periodic RFDEs, the difficulty is that the operator $U(t)$ has no closed form, so no closed-form stability conditions can be expected. Stability investigations are often carried out by numerical simulations (see, for example, Balachandran 2001). Another approach is used by Insperger & Stépán (2000a) when the discrete time delay is approximated by special continuous ones, and the infinite-dimensional eigenvalue problem is transformed into an approximate finite-dimensional one. An alternative of Hill's method was used by Seagalman & Butcher (2000) to determine the stability properties of turning processes with harmonic impedance modulation.

In spite of all these difficulties, the stability chart of the delayed Mathieu equation is constructed in the subsequent sections in an 'almost' closed form. This chart serves as a basic reference for the above engineering applications, and also serves as a test example for numerical methods investigating the stability of linear periodic RFDEs.

2. Special cases

In this section we consider the Mathieu equation and the equation of the delayed oscillator as the two special limit cases of the delayed Mathieu equation.

The Mathieu equation

$$\ddot{x}(t) + (\delta + \varepsilon \cos t)x(t) = 0 \quad (2.1)$$

was first discussed by Mathieu (1868) in connection with the problem of vibrations of an elliptic membrane. For its stability analysis, Hill (1886) worked out a method (the so-called Hill's infinite determinant method) that was generalized by Rayleigh (1887). The most straightforward and less accurate method is the piecewise constant approximation of the periodic coefficient (see, for example, D'Agelo 1970). There are other methods described in the book of Nayfeh & Mook (1979): the Lindstedt–Poincaré technique and the method of multiple scales. A novel approach using Chebyshev polynomials was developed by Sinha & Wu (1991).

The stability chart, the well-known Strutt–Ince diagram, was first published by van der Pol & Strutt (1928). This chart shows the domains of stability and instability denoted by S and $U_{\pm 1}$, respectively, in the (δ, ε) parameter plane of figure 1. S refers

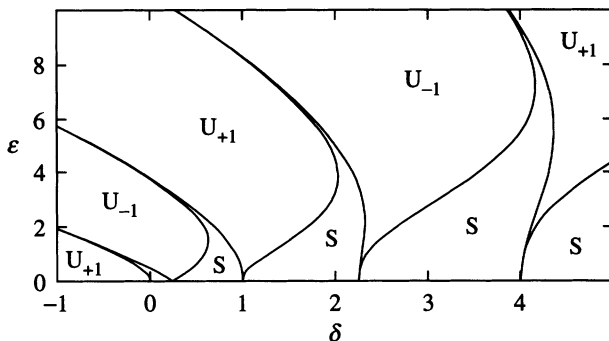


Figure 1. The Strutt-Ince stability chart of (2.1).

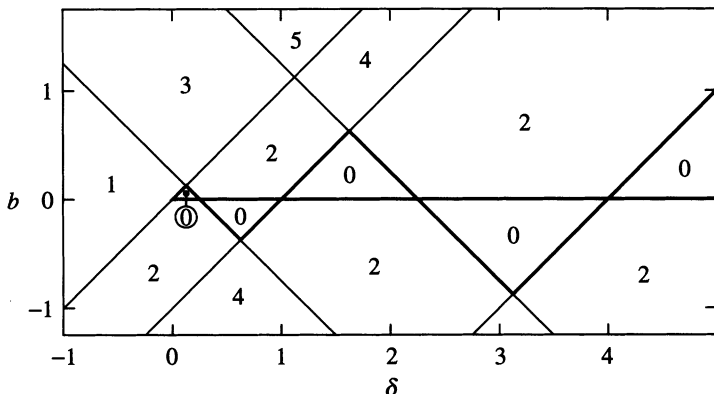


Figure 2. The Hsu-Bhatt-Vyshnegradskii stability chart of (2.2).

to complex conjugate characteristic multipliers on the unit circle, $U_{\pm 1}$ refers to a real characteristic multiplier greater than +1 or less than -1, respectively.

The delayed oscillator is described by the scalar RFDE

$$\ddot{x}(t) + \delta x(t) = bx(t - 2\pi). \tag{2.2}$$

The first attempts to give stability criteria for (2.2) were made by Bellman & Cooke (1963) and by Bhatt & Hsu (1966). They used the D-subdivision method (see Neimark 1949) combined with a theorem of Pontryagin (1942). A more sophisticated method was developed by Stépán (1989), applicable even for the combination of several discrete and continuous time delays.

Although the stability chart (see figure 2) in the parameter plane (δ, b) has a very clear structure. It was first published correctly only in 1966 by Hsu & Bhatt (1966). According to Kolmanovskii & Nosov (1986), this chart was also published in the literature in Russian, often referred there as the Vyshnegradskii diagram. The stability boundaries are lines with slope +1 and -1. The numbers denote the numbers of characteristic roots with positive real parts. This will be called the number of instabilities. If this number is 0, then the corresponding domain refers to an asymptotically stable system. This will be called the domain of stability, bounded by thick lines in the chart of figure 2. The only domains of stability are the triangles attached to the $b = 0$ axis for $\delta > 0$. Along the boundaries where the number of instabilities changes from 0 to 2, *Hopf bifurcations* occur.

3. The delayed Mathieu equation

The equation of interest to us is the delayed Mathieu equation, defined as

$$\ddot{x}(t) + (\delta + \varepsilon \cos t)x(t) = bx(t - 2\pi). \tag{3.1}$$

The time delay is equal to the principal period 2π , so it can also be viewed as a special resonant case of systems with optional principal period. We are looking for the stability chart in the space of the parameters δ, b, ε . The stability charts for the two special cases $\varepsilon = 0$ and $b = 0$ are presented in the previous section. The stability charts in the plane (δ, b) will be determined for various values of the parameter ε . Geometrically, this means that we follow how the stable triangles of figure 2 change for $\varepsilon > 0$.

Let us define the boundary curves as the set of points in the plane (δ, b) , where there is at least one characteristic multiplier in modulus equal to one. The domains bounded by these curves are invariant for the number of instabilities due to the continuous dependence on the parameters.

According to the Floquet theory of RFDEs, we use the trial solution

$$x(t) = p(t)e^{\lambda t} + \bar{p}(t)e^{\bar{\lambda}t}, \tag{3.2}$$

where $p(t) = p(t + 2\pi)$ is a periodic function and λ is the characteristic exponent. Expand the periodic function $p(t)$ in (3.2) into a Fourier series, and substitute

$$x(t) = \sum_{k=-\infty}^{\infty} (C_k e^{(\lambda+ik)t} + \bar{C}_k e^{(\bar{\lambda}-ik)t}) \tag{3.3}$$

into (3.1). The standard balancing of the harmonics $e^{(\lambda+ik)t}$ yields a system of equations for the coefficients C_k :

$$\frac{1}{2}\varepsilon C_{k-1} + c_k C_k + \frac{1}{2}\varepsilon C_{k+1} = 0, \quad k = -\infty, \dots, \infty, \tag{3.4}$$

where

$$c_k = \delta + (\lambda + ik)^2 - b e^{-2\pi(\lambda+ik)}. \tag{3.5}$$

The balancing of the complex conjugate harmonics leads to the same equations for \bar{C}_k . There is a non-trivial solution of system (3.4) if the determinant of the tridiagonal form for the C_k , the so-called Hill's infinite determinant, is zero:

$$D(\lambda, \delta, b, \varepsilon) = \det \begin{pmatrix} \ddots & \ddots & \ddots & & \\ & \frac{1}{2}\varepsilon & c_k & \frac{1}{2}\varepsilon & \\ & & \ddots & \ddots & \ddots \end{pmatrix} = 0. \tag{3.6}$$

This transcendental expression can be treated as the characteristic function of (3.1), since its roots are the characteristic exponents. Consequently, equation (3.6) is equivalent to (1.3) for the characteristic multipliers $\mu = \exp(2\pi\lambda)$.

In order to carry out calculations, only the truncated system of equations of index $k = -N, \dots, N$ will be considered. This approximation is just the same as the one applied during the construction of the Strutt–Ince diagram. In the following, we will construct the boundary curves, then determine the domains of stability.

(a) Boundary curves

According to the D-subdivision method, the substitution of $\lambda = i\omega$ into (3.6) gives an implicit form for the approximate boundary curves of (3.1) in the parameter space (δ, b, ε) with the frequency parameter ω . In this case, the diagonal elements in (3.6) read

$$c_k = \delta - (\omega + k)^2 - be^{-i2\pi\omega}. \tag{3.7}$$

Note that the imaginary part of c_k is not dependent on k :

$$\text{Im } c_k = b \sin(2\pi\omega), \quad k = -N, \dots, N. \tag{3.8}$$

We disregard the case $b = 0$, which gives the classical Mathieu equation. Then we can state that $\text{Im } c_k = 0$ if and only if $\omega = \frac{1}{2}j$, where $j = 0, 1, \dots$. Now we examine two cases.

Case 1 ($\omega \neq \frac{1}{2}j, j = 0, 1, \dots$)

In this case, $\text{Im } c_k \neq 0$ for any k , as follows from (3.8). The Gauss algorithm can be applied for the tridiagonal matrix in (3.6) to transform it to an upper triangular matrix having elements d_k in the main diagonal. Clearly, $d_{-N} = c_{-N} \neq 0$. In the $(N + k)$ th step of the Gauss elimination process, Hill’s matrix assumes the form

$$\begin{pmatrix} d_{-N} & \frac{1}{2}\varepsilon & 0 & \dots & & & & & \\ \vdots & \ddots & \ddots & \ddots & & & & & \\ \dots & 0 & d_{k-1} & \frac{1}{2}\varepsilon & 0 & \dots & & & \\ & \dots & 0 & d_k & \frac{1}{2}\varepsilon & 0 & \dots & & \\ & & \dots & 0 & \frac{1}{2}\varepsilon & c_{k+1} & \frac{1}{2}\varepsilon & 0 & \dots \\ & & & \dots & 0 & \frac{1}{2}\varepsilon & c_{k+2} & \frac{1}{2}\varepsilon & 0 & \dots \\ & & & & & \ddots & \ddots & \ddots & \ddots & \ddots \end{pmatrix}. \tag{3.9}$$

Let us suppose that $\text{sgn}(\text{Im } d_k) = \text{sgn}(\text{Im } c_k)$ for some k . Since $\text{Im } c_k \neq 0$, this means that $\text{Im } d_k \neq 0$, i.e. $|d_k| \neq 0$. Thus the subsequent elimination of $\frac{1}{2}\varepsilon$ in front of c_{k+1} leads to

$$d_{k+1} = c_{k+1} - \frac{\varepsilon^2}{4d_k} = \left(\text{Re } c_{k+1} - \frac{\varepsilon^2 \text{Re } d_k}{4|d_k|^2} \right) + i \left(\text{Im } c_{k+1} + \frac{\varepsilon^2 \text{Im } d_k}{4|d_k|^2} \right). \tag{3.10}$$

Consequently,

$$\text{sgn}(\text{Im } d_{k+1}) = \text{sgn} \left(\text{Im } c_{k+1} + \left(\frac{\varepsilon}{2|d_k|} \right)^2 \text{Im } d_k \right) = \text{sgn}(\text{Im } d_k) = \text{sgn}(\text{Im } c_k) \neq 0. \tag{3.11}$$

Since $\text{Im } d_{-N} = \text{Im } c_{-N} = b \sin(2\pi\omega) \neq 0$, we have $\text{Im } d_k \neq 0$, that is, $|d_k| \neq 0$ is true by induction.

The determinant of Hill’s matrix can be calculated as the product of the diagonal elements of the upper triangular matrix. Hence

$$D(i\omega, \delta, b, \varepsilon) = \prod_{k=-N}^N d_k \neq 0, \tag{3.12}$$

and condition (3.6) cannot be satisfied.

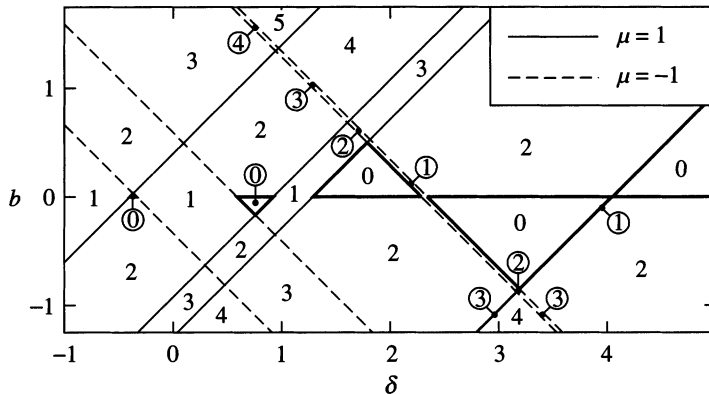


Figure 3. Domains of stability of (3.1) for $\varepsilon = 1$ (denoted by zeros).

This means that there is no non-trivial solution of system (3.4), and there are no boundary curves in this case.

Case 2 ($\omega = \frac{1}{2}j, j = 0, 1, \dots$)

In this case, the diagonal elements in (3.6) are real:

$$c_k = \delta - (k + \frac{1}{2}j)^2 - b(-1)^j. \tag{3.13}$$

If j is even, that is, $j = 2h, h = 0, 1, \dots$, then $\lambda = ih$, and the corresponding characteristic multiplier is

$$\mu = e^{ih2\pi} = e^{i2\pi} = 1. \tag{3.14}$$

In this case, $c_k = \delta - b - (k + h)^2$, and (3.6) gives the relation $f_{+1}(\delta - b, \varepsilon) = 0$ for the boundary curves. For the case $b = 0$, the relation $f_{+1}(\delta, \varepsilon) = 0$ serves the $\mu = +1$ stability boundary curves of the classical Mathieu equation defined in the form $\delta = g_{+1}(\varepsilon)$, as was shown first by van der Pol & Strutt (1928). This means that the boundary curves exist for the $b \neq 0$ case, too, in the form $\delta - b = g_{+1}(\varepsilon)$. In the plane (δ, b) , these are lines with slope +1 (represented by solid lines in figure 3). Along these boundary curves, there exists a characteristic multiplier $\mu = +1$, and (3.1) has a periodic solution of period 2π . This case is topologically equivalent to the *saddle-node bifurcation* of autonomous systems.

If j is odd, that is, $j = 2h+1, h = 0, 1, \dots$, then $\lambda = i(h + \frac{1}{2})$ and the corresponding characteristic multiplier is

$$\mu = e^{i(h+1/2)2\pi} = e^{i\pi} = -1. \tag{3.15}$$

In this case, $c_k = \delta + b - (k + h + \frac{1}{2})^2$, and (3.6) implies the boundary curve relation $f_{-1}(\delta + b, \varepsilon) = 0$. For the same reason as above, the boundary curves exist again in the form $\delta - b = g_{-1}(\varepsilon)$, where $\delta = g_{-1}(\varepsilon)$ gives the $\mu = -1$ stability boundary curves of the classical Mathieu equation. The boundary curves are lines with slope -1 in the parameter plane (δ, b) (represented by dashed lines in figure 3). Along these boundary curves, there exists a characteristic multiplier $\mu = -1$, and (3.1) has a non-trivial periodic solution of period 4π . This type of bifurcation is called *period doubling*, or *flip bifurcation*. There is no topologically equivalent type of bifurcation for autonomous systems.

Thus the boundary curves are lines in the plane (δ, b) . For varying parameter ε , these lines pass along the boundary curves of the Strutt–Ince diagram. As mentioned before, these charts are approximate to the same extent as the Strutt–Ince diagram ($N = 20$ in the figures), and they converge to the exact result for the $N \rightarrow \infty$ limit case. This means that the appearance of the delay in the Mathieu equation does not require any more approximation in the stability analysis, just the same as already used in the classical Mathieu equation. The point is that the parametric excitation in the delayed oscillator does not alter the linearity of the stability boundaries.

(b) Domains of stability

Since the characteristic multipliers and exponents depend continuously on the system parameters, the number of instabilities is constant in each domain separated by the boundary curves. The special case $\varepsilon = 0$ can be treated as a reference regarding the number of instabilities. The domains attached to these triangles of stability in the stability chart of figure 2 also have zero instability number. Similarly, some domains of instability can also be identified this way, and also the number of instabilities can be given based on the $\varepsilon = 0$ chart. But there are also some new domains, which are not connected directly to any domain of the chart $\varepsilon = 0$ in figure 2. To decide the stability of these domains, the sign of $\text{Re } \lambda$ will be investigated near to the boundary curves. The derivative of λ with respect to the parameter b will be determined for $\lambda = \frac{1}{2}ij, j = 0, 1, \dots$

A recursive form for the calculation of the tridiagonal upper-left sub-determinants in (3.6) can be given as

$$D_{-N} = c_{-N}, \tag{3.16}$$

$$D_{-N+1} = c_{-N}c_{-N+1} - \frac{1}{4}\varepsilon^2, \tag{3.17}$$

$$D_k = c_k D_{k-1} - \frac{1}{4}\varepsilon^2 D_{k-2}, \quad k = -N + 2, \dots, N. \tag{3.18}$$

Let us denote the partial derivative with respect to b by a prime ($\square' = \partial \square / \partial b$) and the substitution of $\lambda = \frac{1}{2}ij$ by a hat ($\hat{\square} = \square|_{\lambda=ij/2}$). According to this notation, the partial derivatives of expressions (3.5), (3.16) and (3.17) yield

$$c'_k = 2(\lambda + ik)\lambda' - e^{-(\lambda+ik)2\pi} + b2\pi\lambda' e^{-(\lambda+ik)2\pi}, \tag{3.19}$$

$$\hat{c}'_k = (2\pi b(-1)^j + i(j + 2k))\lambda' - (-1)^j, \tag{3.20}$$

$$\hat{D}'_{-N} = (2\pi b(-1)^j \Gamma_{-N} + i\Omega_{-N})\lambda' - (-1)^j \Gamma_{-N}, \tag{3.21}$$

$$\hat{D}'_{-N+1} = (2\pi b(-1)^j \Gamma_{-N+1} + i\Omega_{-N+1})\lambda' - (-1)^j \Gamma_{-N+1}, \tag{3.22}$$

where the coefficients

$$\Gamma_{-N} = 1,$$

$$\Omega_{-N} = j - 2N,$$

$$\Gamma_{-N+1} = \hat{c}_{-N} + \hat{c}_{-N+1},$$

$$\Omega_{-N+1} = \hat{c}_{-N}(j - 2N + 2) + \hat{c}_{-N+1}(j - 2N)$$

are real numbers, since \hat{c}_k is real for all $k = -N, \dots, N$. The same differentiation of (3.18) yields the recursion

$$\hat{D}'_k = \hat{c}'_k \hat{D}_{k-1} + \hat{c}_k \hat{D}'_{k-1} - \frac{1}{4}\varepsilon^2 \hat{D}'_{k-2}, \quad k = -N + 2, \dots, N. \tag{3.23}$$

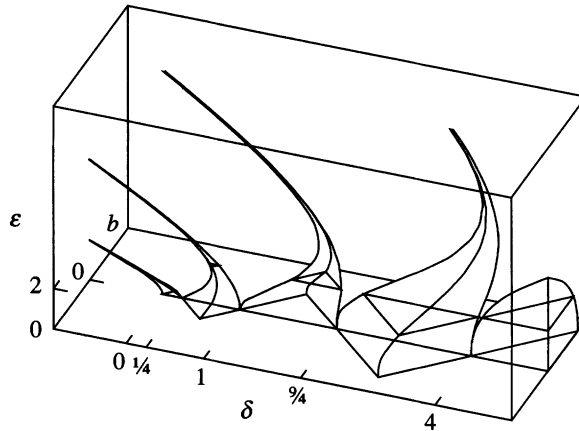


Figure 4. Stability chart of the delayed Mathieu equation.

We prove by induction that (3.23) can be expressed in the same form as (3.21) and (3.22). For some k , let us suppose that

$$\hat{D}'_{k-2} = (2\pi b(-1)^j \Gamma_{k-2} + i\Omega_{k-2})\lambda' - (-1)^j \Gamma_{k-2}, \tag{3.24}$$

$$\hat{D}'_{k-1} = (2\pi b(-1)^j \Gamma_{k-1} + i\Omega_{k-1})\lambda' - (-1)^j \Gamma_{k-1}, \tag{3.25}$$

where $\Gamma_{k-2}, \Gamma_{k-1}, \Omega_{k-2}, \Omega_{k-1}$ are real numbers. Then, using (3.20), equation (3.23) reads

$$\hat{D}'_k = (2\pi b(-1)^j \Gamma_k + i\Omega_k)\lambda' - (-1)^j \Gamma_k, \quad k = -N + 2, \dots, N, \tag{3.26}$$

where the coefficients

$$\begin{aligned} \Gamma_k &= \hat{D}_{k-1} + \Gamma_{k-1}\hat{c}_k - \frac{1}{4}\varepsilon^2 \Gamma_{k-2}, \\ \Omega_k &= (j + 2k)\hat{D}_{k-1} + \Omega_{k-1}\hat{c}_k - \frac{1}{4}\varepsilon^2 \Omega_{k-2} \end{aligned}$$

are real numbers, again. Together with (3.21) and (3.22), this completes the induction.

The final round of recursion is given by the $k = N$ case. The implicit differentiation of the characteristic exponent in $\hat{D}'_N = 0$ provides the expression of $\text{Re } \lambda'$ after a straightforward algebraic calculation from (3.26):

$$\text{Re } \lambda' = \frac{2\pi \Gamma_N^2}{(2\pi b(-1)^j \Gamma_N)^2 + \Omega_N^2} b. \tag{3.27}$$

Since the coefficient of b is positive, $\text{sgn}(\text{Re } \lambda') = \text{sgn}(b)$ on the boundary curves. That is, moving away from the $b = 0$ axis, each boundary line represents at least one characteristic exponent becoming unstable (i.e. crossing the imaginary axis of the complex plane from the left to the right). So the only domains of stability are the triangles born from the stable triangles of the $\varepsilon = 0$ case. Since the case $\varepsilon = 0$ is already known (see figure 2), the number of instabilities can be determined for all the domains by (3.27) and topological considerations (see the numbers in the chart of figure 3). The domains of stability are bounded by thick lines. The frame of the three-dimensional stability chart in the space (δ, b, ε) is shown in figure 4.

4. Conclusions

The closed form three-dimensional stability chart for the delayed Mathieu equation (3.1) was constructed. It was shown analytically that the boundary curves in the plane (δ, b) are lines for any ε . The number of instabilities was also determined in the domains separated by these lines. At the boundaries with slope $+1$, a characteristic multiplier crosses the unit circle at $+1$, presenting a 2π -periodic motion. At the boundaries with slope -1 , a characteristic multiplier crosses the unit circle at -1 , presenting a 4π -periodic motion (a *period-doubling bifurcation*).

This research was supported by the Hungarian National Science Foundation under grant no. OTKA T030762/99, and the Ministry of Education and Culture grant no. MKM FKPP 0380/97.

References

- Balachandran, B. 2001 Nonlinear dynamics of milling process. *Phil. Trans. R. Soc. Lond. A* **359**, 793–820.
- Bayly, P. V., Halley, J. E., Mann, B. P. & Davies, M. A. 2001 Stability of interrupted cutting by temporal finite element analysis. In *Proc. ASME 2001 Design Engineering Technical Conf., Pittsburgh, PA*, paper no. DETC2001/VIB-21581.
- Bellman, R. & Cooke, K. 1963 *Differential-difference equations*. Academic.
- Bhatt, S. J. & Hsu, C. S. 1966 Stability criteria for second-order dynamical systems with time lag. *J. Appl. Mech.* **33**, 113–118.
- D'Agelo, H. 1970 *Linear time-varying system: analysis and synthesis*. Boston, MA: Allyn and Bacon.
- Davies, M. A., Pratt, J. R., Dutterer, B. & Burns, T. J. 2002 Stability prediction for low radial immersion milling. *J. Manufacturing Sci. Engng* **124**, 117–125.
- Farkas, M. 1994 *Periodic motions*. Springer.
- Floquet, M. G. 1883 Équations différentielles linéaires a coefficients périodiques. *Annls Scient. École Norm. Sup.* **12**, 47–89.
- Hale, J. K. 1977 *Theory of functional differential equations*. Springer.
- Hale, J. K. & Lunel, S. M. V. 1993 *Introduction to functional differential equations*. Springer.
- Hill, G. W. 1886 On the part of the motion of the lunar perigee which is a function of the mean motions of the Sun and Moon. *Acta Math.* **8**, 1–36.
- Hsu, C. S. & Bhatt, S. J. 1966 Stability charts for second-order dynamical systems with time lag. *J. Appl. Mech.* **33**, 119–124.
- Inspurger, T. & Stépán, G. 2000a Stability of the milling process. *Periodica Polytechnica* **44**, 47–57.
- Inspurger, T. & Stépán, G. 2000b Remote control of periodic robot motion. In *Proc. 13th Symp. on Theory and Practice of Robots and Manipulators* (ed. A. Morecki, G. Bianchi & C. Rzymkowsky), pp. 197–203. Springer.
- Kolmanovskii, V. B. & Nosov, V. R. 1986 *Stability of functional differential equations*. Academic.
- Mathieu, E. 1868 Mémoire sur le mouvement vibratoire d'une membrane de forme elliptique. *J. Math.* **13**, 137–203.
- Nayfeh, A. H. & Mook, D. T. 1979 *Nonlinear oscillations*. Wiley.
- Neimark, Ju. I. 1949 D-subdivision and spaces of quasi-polynomials. *Prikl. Mat. Mech.* **13**, 349–380. (In Russian.)
- Pontryagin, L. S. 1942 On the zeros of some elementary transcendental functions. *Izv. Akad. Nauk SSSR* **6**, 115–134. (In Russian.)

- Rayleigh, J. W. 1887 On the maintenance of vibrations by forces of double frequency, and on the propagation of waves through a medium endowed with a periodic structure. *Phil. Mag. J. Sci.* **24**, 145–159.
- Seagalman, D. J. & Butcher, E. A. 2000 Suppression of regenerative chatter via impedance modulation. *J. Vib. Control* **6**, 243–256.
- Sinha, S. C. & Wu, D. H. 1991 An efficient computational scheme for the analysis of periodic systems. *J. Sound Vib.* **151**, 91–117.
- Stépán, G. 1989 *Retarded dynamical systems*. New York: Longman.
- van der Pol, F. & Strutt, M. J. O. 1928 On the stability of the solutions of Mathieu's equation. *Phil. Mag. J. Sci.* **5**, 18–38.